

Article

Investigating the Molecular Mechanism of Qianghuo Shengshi Decoction in the Treatment of Ankylosing Spondylitis Based on Network Pharmacology and Molecular Docking Analysis

Simin Luo, Xiang Xiao, Wenting Luo, Xuan Zhang, Jian Zhang and Songqi Tang *

College of Traditional Chinese Medicine, Hainan Medical University, Haikou 571199, China; luosimin1111@gmail.com (S.L.); xiaoxianghainmc@gmail.com (X.X.); luowentinghainmc@gmail.com (W.L.); zhangxuanhainmc@gmail.com (X.Z.); zhangj1995666@163.com (J.Z.)

* Correspondence: tangsongqi@hainmc.edu.cn

Abstract: Background: Qianghuo Shengshi decoction (QHSSD), a traditional Chinese medicine formula, is used to treat ankylosing spondylitis (AS) in China. The pharmacological mechanism of QHSSD for AS remains to be clarified. In this study, we investigated the molecular mechanisms of QHSSD in the treatment of AS using network pharmacology and molecular docking. Methods: To obtain the chemical components and potential targets of QHSSD, we used the Traditional Chinese Medicine Systematic Pharmacology Database and Analysis Platform (TCMSP) and SwissTargetPrediction. AS potential targets were found in the GeneCards, OMIM, and DisGenets databases. A Venn diagram was used to screen QHSSD and AS common potential targets. The STRING website and Cytoscape software were used to create and analyze protein–protein interactions and component–target networks. The DAVID database was used for the gene ontology (GO) function and Kyoto Encyclopedia of Genes and Genomes (KEGG) pathway enrichment analysis. Molecular docking was used to visualize drug–target interactions. Results: The component–target network consisted of 119 chemical components and 193 potential targets. QHSSD was implicated in various biological processes, such as inflammation and angiogenesis, and mediated multiple signaling pathways, such as the MAPK signaling pathway. Molecular docking revealed good binding ability between medicarpin, notoptol, vitetrifolin E, and cnidilin and EGFR, TNF- α , ALB, and VEGFA. Conclusions: The chemical compositions, potential targets, and pathways involved in the QHSSD treatment of AS were successfully predicted in this study. This study provides a solid foundation for the selection of drugs to treat AS.

Keywords: ankylosing spondylitis; network pharmacology; molecular docking; Traditional Chinese Medicine



Citation: Luo, S.; Xiao, X.; Luo, W.; Zhang, X.; Zhang, J.; Tang, S. Investigating the Molecular Mechanism of Qianghuo Shengshi Decoction in the Treatment of Ankylosing Spondylitis Based on Network Pharmacology and Molecular Docking Analysis. *Processes* **2022**, *10*, 1487. <https://doi.org/10.3390/pr10081487>

Academic Editor: Jing Tang

Received: 27 June 2022

Accepted: 25 July 2022

Published: 28 July 2022

Publisher's Note: MDPI stays neutral with regard to jurisdictional claims in published maps and institutional affiliations.



Copyright: © 2022 by the authors. Licensee MDPI, Basel, Switzerland. This article is an open access article distributed under the terms and conditions of the Creative Commons Attribution (CC BY) license (<https://creativecommons.org/licenses/by/4.0/>).

1. Introduction

Ankylosing spondylitis (AS) is a prevalent spondyloarthropathy, a chronic inflammatory autoimmune disease that affects the joints of the spine and produces significant persistent pain [1]. Immune cells and innate cytokines, particularly human leukocyte antigen (HLA)-B27 and the interleukin-23/17 axis, have been discovered to play a critical role in the pathogenesis of AS [2]. This disease is developing in a worldwide epidemiological trend, with some variance between races and areas. The frequency of AS is 0.26 percent in China [3]. Patients with AS must quit working after an average of 15.6 years, with the majority of functional loss occurring during the first 10 years. AS progresses at different rates, with around a third of people attaining severe impairment. Lower back pain, stiffness, restricted chest expansion, and limited spinal movement are common early on, and they are commonly accompanied by weariness [4–7]. NSAIDs and tumor necrosis factor antagonists are currently recommended for the treatment of AS according to current guidelines. In individuals with peripheral joint involvement, traditional synthetic disease-modifying

anti-rheumatic medications such as sulphasalazine and methotrexate are suggested [8]. However, long-term usage may pose cardiovascular, gastrointestinal, and renal hazards [9], and the high cost of some medicines places a significant financial burden on patients.

Throughout its long history, Traditional Chinese Medicine (TCM) has amassed a vast amount of clinical expertise in the prevention and treatment of this illness. AS is caused by wind, cold, and moisture according to TCM. Because of its capacity to expel wind, eliminate moisture, and reduce pain, Qianghuo Shengshi decoction (QHSSD) is frequently used to treat AS. QHSSD is mainly comprised of Qianghuo (QH), Duhuo (DH), Chuanxiong (CX), Gaoben (GB), Fangfeng (FF), Manjingzi (MJZ), and Gancao (GC).

Network pharmacology is centered on building a component–target network to anticipate the mechanism of action of medications for the treatment of illnesses at the molecular level, using data visualization and analysis. It compensates for the “single ingredient, single target, single medication, single illness” model’s flaws. Molecular docking technology is a computer-assisted analysis that predicts a novel chemical entity or drug’s binding affinity based on its chemical structure. It predicts how a chemical will interact with a given receptor. To understand the mechanism of action of QHSSD for the treatment of AS, a network pharmacology method was employed in this study to anticipate the chemical components, potential targets of action, and critical pathways, and simultaneous simulation and validation were utilized to investigate the molecular docking methods. The workflow is displayed in Figure 1.

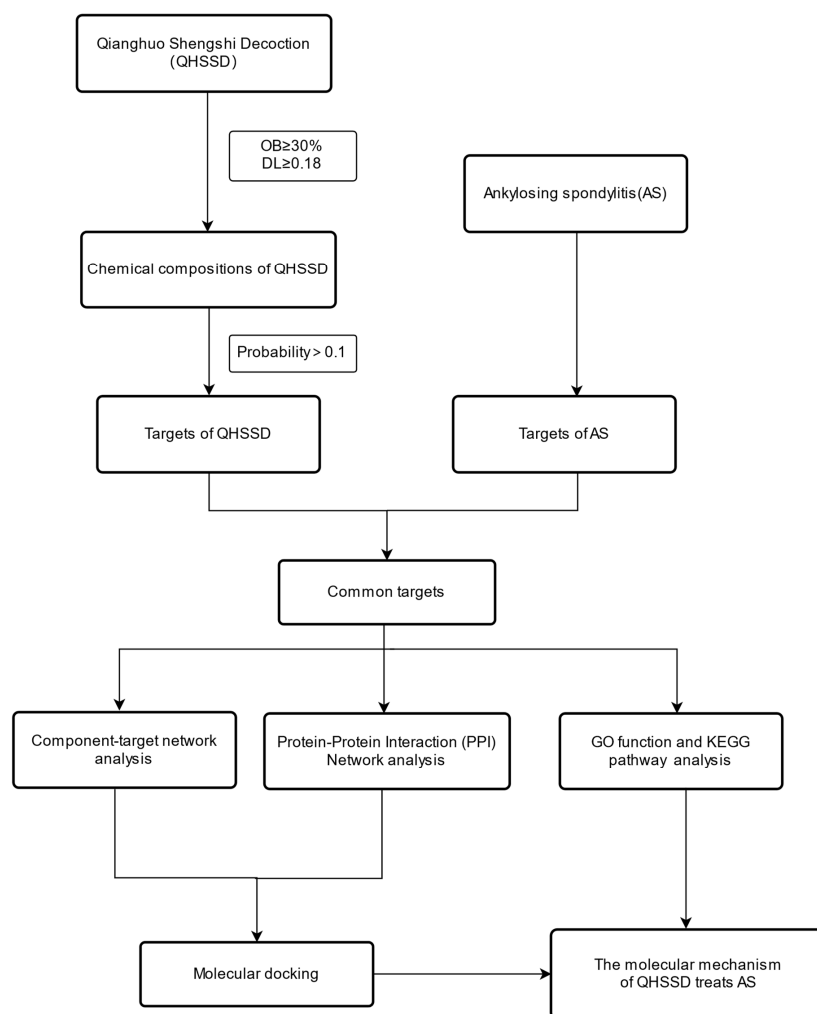


Figure 1. The workflow of the network pharmacology study of QHSSD for AS. Steps mainly included search and screening of potential targets, construction of protein–protein interaction network and component–target network, GO function and KEGG pathway analysis, and molecular docking validation.

2. Methods

2.1. Obtaining the Chemical Components and Target of QHSSD

The Traditional Chinese Medicine Systematic Pharmacology Database and Analysis Platform (TCMSP, <https://tcmsp-e.com/> (accessed on 10 April 2022)) contains 499 plants and their chemical components. More detailed information on each composition's absorption, distribution, metabolism, and efflux (ADME) characteristics in humans are provided. Therefore, the chemical composition of QHSSD was retrieved using TCMSP. One important condition for oral medication research and clinical use is the degree of drug dispersion in the bloodstream. Furthermore, the structural resemblance of compounds in drug databases to clinical therapies is assessed using drug-like (DL) characteristics. Therefore, the chemical components were evaluated based on oral bioavailability (OB) > 30% and DL > 0.18 [10–12]. Pubchem (<https://pubchem.ncbi.nlm.nih.gov/> (accessed on 10 April 2022)) was used to convert the screening findings into Canonical SMILES. To anticipate the chemical component potential targets, we utilized SwissTargetPrediction (<http://www.swisstargetprediction.ch/> (accessed on 15 April 2022)). Duplicates were deleted after integration. Potential targets with a prediction score larger than 0.1 were chosen as QHSSD chemical component potential targets [13].

2.2. Obtaining the Potential Targets of AS

The Human Gene Database (GeneCards, <https://www.genecards.org/> (accessed on 20 April 2022)) is a gene-centric database that combines data from 125 sources on 152,704 human genes, encompassing over 90% of all human protein-coding genes [14]. The Online Human Mendelian Inheritance Database (OMIM, <https://www.omim.org/> (accessed on 20 April 2022)) collects data on genes and genetic traits, as well as their interactions [15]. The DisGeNET database (<https://www.disgenet.org/> (accessed on 20 April 2022)) is a knowledge platform built on a comprehensive catalog of disease-related genes and variants. It combines data on genes and variations linked to human illnesses from a variety of sources and uses text mining to pull information from scholarly publications [16]. The GeneCards, OMIM, and DisGeNET databases were utilized to search for AS and to filter and gather disease potential targets using the search phrase “Ankylosing spondylitis”.

2.3. Obtaining Common Potential Targets of QHSSD and AS

To obtain common potential targets of QHSSD and AS, the QHSSD and AS potential targets were imported into a Venn diagram.

2.4. Network Construction

2.4.1. Construction of Component–Target Interaction Network

To create a network diagram to depict the complex component–target interactions, the QHSSD chemical components and their intersecting potential targets with ankylosing spondylitis were loaded into Cytoscape 3.8.2 software (<https://www.cytoscape.org/> (accessed on 25 April 2022)). This software was created by the American Institute of Systems Biology (Seattle, WA, USA).

2.4.2. Construction of Protein–Protein Interaction Network

The STRING database (<https://string-db.org/> (accessed on 30 April 2022)) is a resource for studying protein interactions (PPI). The database was used to construct a protein–protein interaction network for the QHSSD and AS common potential targets. The organism was set to “Homo sapiens,” with a confidence level of 0.4 [17]. The PPI network was then created by hiding the individual potential targets in the network. Cytoscape 3.8.2 software was used to conduct the network analysis.

2.5. Gene Ontology (GO) Function and Kyoto Encyclopedia of Genes and Genomes (KEGG) Pathway Analysis

The DAVID database (<https://david.ncifcrf.gov/> (accessed on 30 April 2022)) was used to perform the gene ontology (GO) function and Kyoto Encyclopedia of Genes and Genomes (KEGG) pathway enrichment analysis. “OFFICIAL GENE SYMBOL” was chosen as the select identifier, “Gene List” was chosen as the list type, and “Homo sapiens” was chosen the species. Other settings were set to default. A p value < 0.05 was used as the filtering criterion. The DAVID database uses Fisher’s test. Fisher’s exact p -values are computed by summing probabilities p over defined sets of tables ($\text{Prob} = \sum Ap$) [18]. To generate enrichment bubble plots, the enrichment analysis was carried out using the microbiology platform (<http://www.bioinformatics.com.cn/> (accessed on 30 April 2022)).

2.6. Molecular Docking

The Pubchem database was used to obtain the tertiary structure file with core chemical components suffixed with sdf. The PDB database (<https://www.rcsb.org/> (accessed on 1 May 2022)) was used to obtain the structure file with the target protein suffixed with pdb. The ligand was the core chemical component of QHSSD, while the receptor was the AS core target. In terms of predicting binding locations and binding conformations, CB-Dock (<http://clab.labshare.cn/cb-dock/php/> (accessed on 1 May 2022)) beats other state-of-the-art blind docking programs [19]. Therefore, CB-Dock was used in this investigation for molecular docking. The lower the receptor’s free binding energy to the ligand, the more stable it is. The greater the ligand molecule’s binding activity to the target protein, the better.

3. Results

3.1. The Chemical Components and Potential Targets of QHSSD

After screening and integrating, the search yielded a total of 154 QHSSD chemical components (Supplementary Table S1). For QH, DH, CX, GB, FF, MJZ, and GC, respectively, 15, 9, 7, 1, 18, 27, and 92 components were obtained. Following the elimination of chemical components with unknown targets, 119 chemical components remained. A total of 899 potential targets were found for QHSSD after screening pharmacological potential targets with a probability greater than 0.1.

3.2. The Potential Targets of AS

The GeneCards, OMIM, and Disgenets databases were used to obtain 2175, 36, and 710 AS-related potential targets, respectively. A total of 2459 potential targets were obtained for AS by deleting the duplicate potential targets.

3.3. Common Potential Targets of QHSSD and AS

The AS potential targets and the QHSSD chemical composition potential targets were loaded into the Venn diagram. A total of 193 common drug–disease potential targets were identified pertaining to QHSSD for the treatment of AS (Figure 2) (Supplementary Table S2).

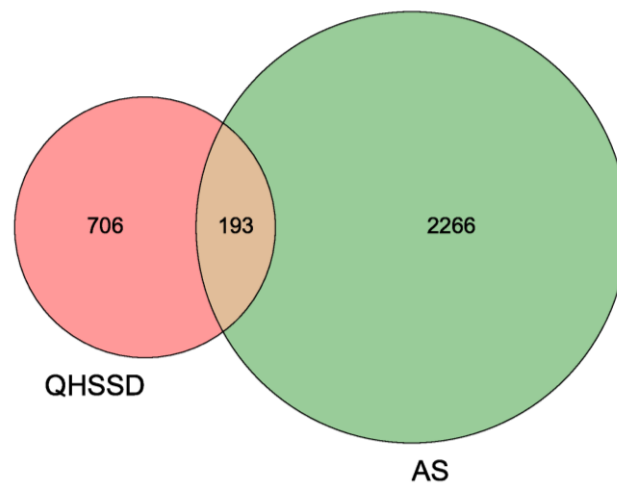


Figure 2. Overlapping potential targets between QHSSD and AS.

3.4. Network Construction

3.4.1. Component–Target Interaction Network

In total, 119 chemical components and 193 common potential targets were imported into Cytoscape 3.8.2 software. The “component–target” interaction network was drawn (Figure 3). The network analysis plugin was used to count the nodes in the network map and examine their connectedness according to the node degree; the higher the node degree, the more biological functions the node has in the network. A network analysis of the graph showed that the top four active components in terms of degree were MOL002565 (medicarpin), MOL011975 (notoptol), MOL011931 (vitetrifolin E), and MOL001956 (cnidilin). Their degrees were 34, 33, 32, and 32, respectively.

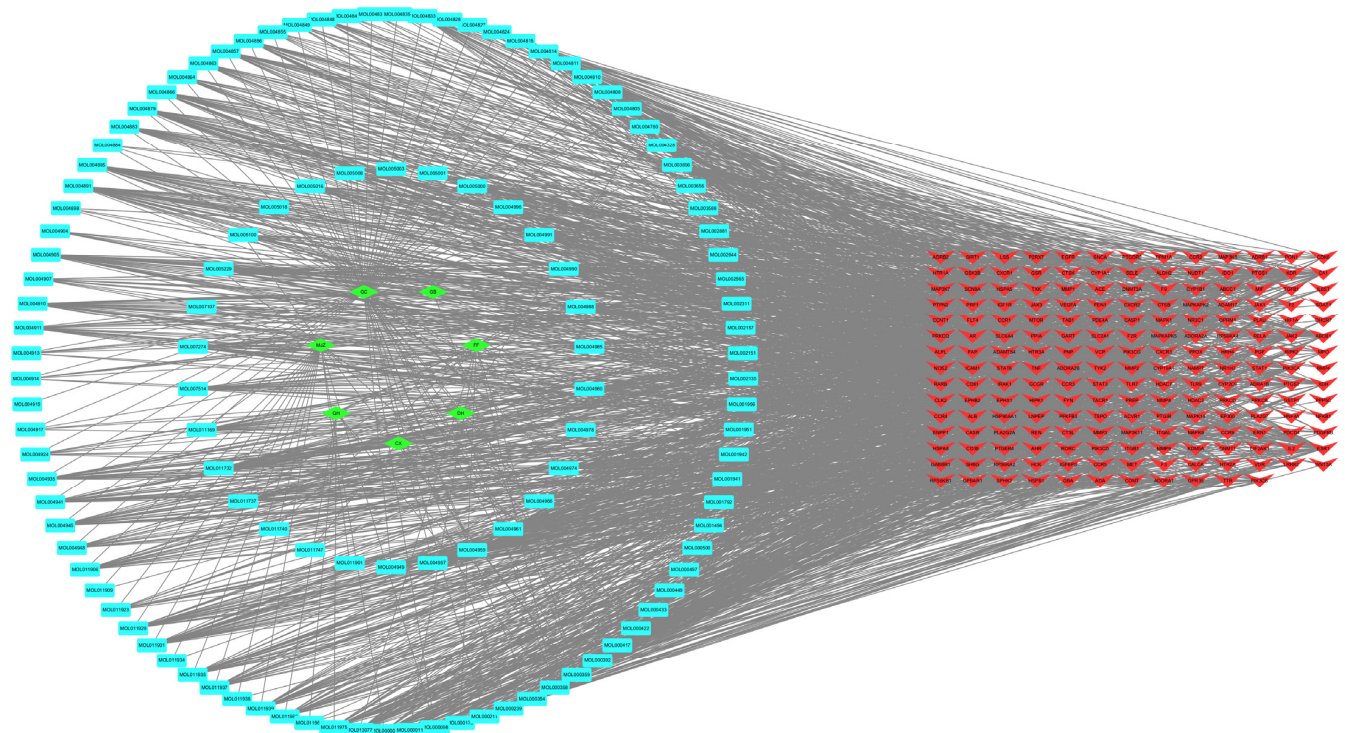
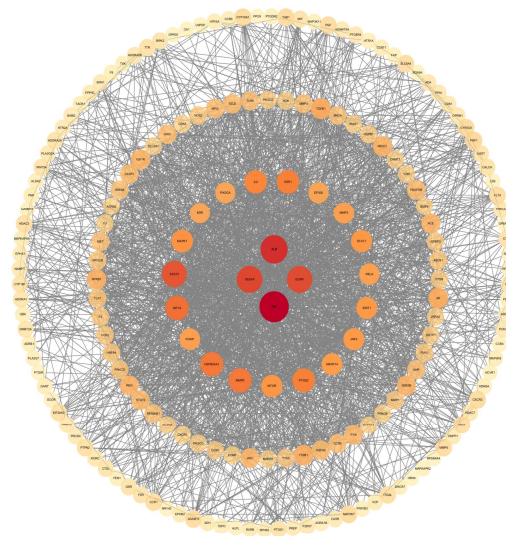


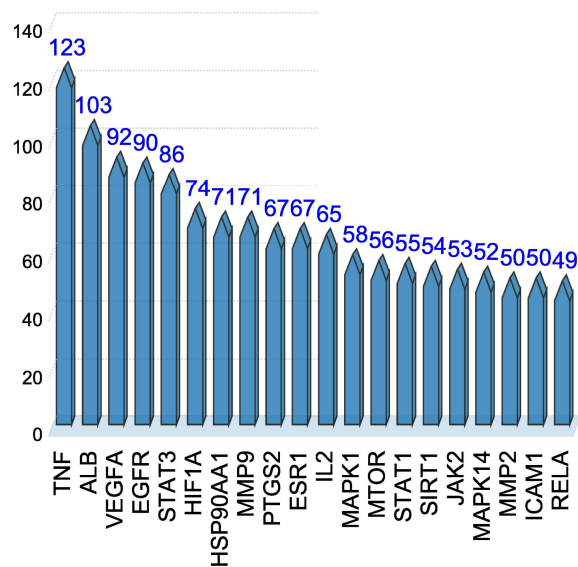
Figure 3. Component–target interaction network (green diamond: QHSSD drugs; blue rectangle: QHSSD chemical compositions; red arrow: common potential targets of QHSSD and AS).

3.4.2. PPI Network

To construct the PPI network, the 193 potential targets were imported into the String database. Individual targets were buried, and the remaining parameters were left constant, with a protein interaction composite score > 0.4. To analyze the PPI network, data were imported into Cytoscape 3.8.2 software. As a result, we obtained PPI network information (Figure 4A), wherein nodes indicate proteins and lines between nodes show protein interactions. The top 20 findings were displayed as 3D bar graphs after being ranked by degree size (Figure 4B). The four potential targets with the darkest colors were tumor necrosis factor-alpha (TNF- α), serum albumin (ALB), vascular endothelial growth factor A (VEGFA), and epidermal growth factor receptor (EGFR). Their degrees were 123, 103, 92, and 90, respectively.



A



B

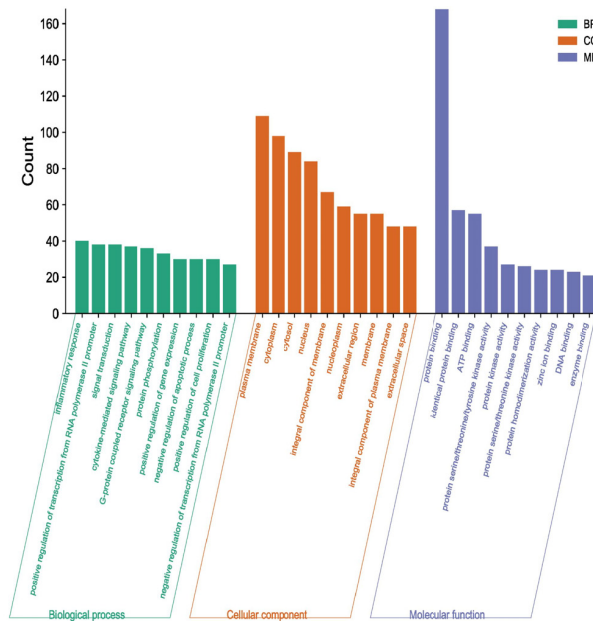
Figure 4. PPI network and 3D bar graphs. (A) PPI network (the size and color depth of the nodes are correlated with their degree), (B) 3D bar graphs of the top 20 targets.

3.5. GO Function and KEGG Pathways Analysis

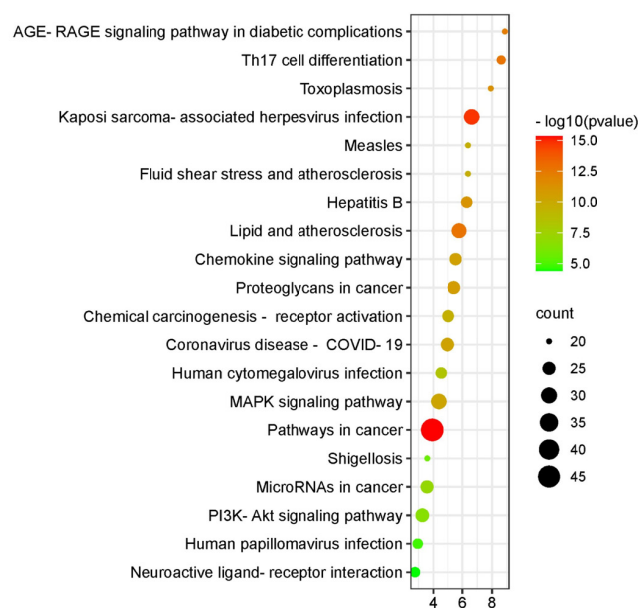
3.5.1. GO Function Analysis

The intersecting gene collection was enriched to a total of 541 biological pathways, mainly including inflammatory response, the positive regulation of transcription from RNA polymerase II promoters, and signal transduction. Additionally, the intersecting gene collection was enriched to a total of 62 cellular components, mainly involving the cytoplasm, cytosol, nucleus, integral component of membrane, and nucleoplasm, and a total of 117 processes associated with molecular function, mainly protein binding, identical protein binding, ATP binding, protein kinase activity, protein serine/threonine kinase activity, protein tyrosine kinase activity, protein homodimerization activity, zinc ion binding, DNA binding, and enzyme binding.

(Figure 5A).



A



B

Figure 5. GO function and KEGG pathways analysis enrichment. (A) GO function (BP: biological process; CC: cellular component; MF: molecular function); (B) KEGG pathways enrichment bubble plots.

3.5.2. KEGG Pathways Analysis

After setting a p value < 0.05 , 137 signaling pathways were discovered through screening. The count was sorted from largest to pairwise smallest. The results of the top 20 enriched pathways are shown in Figure 5B, with $-\log_{10}(p \text{ value})$ indicating enrichment. Pathways involved in cancer, the MAPK signaling pathway, the PI3K-Akt signaling pathway, and other pathways were all associated with inflammation.

3.6. Molecular Docking

The structures of the first four protein targets were obtained in the PDB, including EGFR (PDBID: 6VH4), TNF- α (PDBID: 2az5), ALB (PDBID: 6m4r), and VEGFA (PDBID: 6d3o). They were taken as the core targets of QHSSD for the treatment of AS. The first four were taken as the core chemical ingredients in the chemical composition. After molecular docking, all docking Vina scores were less than -5 (Figure 6, Table 1). The simulation maps of docking showed that the core targets could bind to the core component (Figure 7).

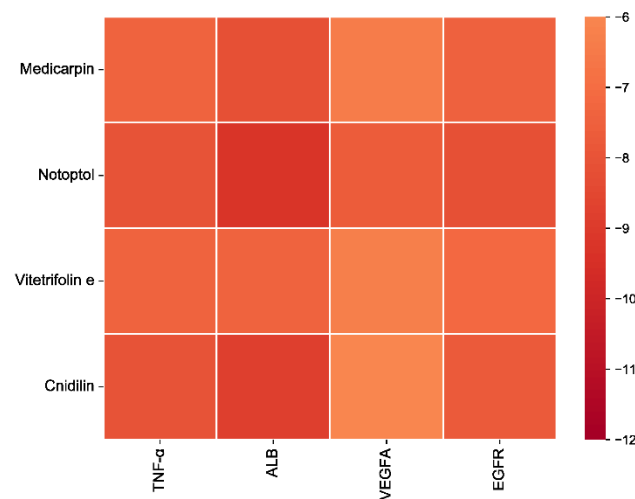


Figure 6. The heat map of the docking Vina scores.

Table 1. Molecular docking parameters and results for the composition of QHSSD and its targets.

Molecule ID	Molecule Name	Target Name	Vina Score	Cavity Size	Center			Size		
					x	y	z	x	y	z
MOL002565	Medicarpin	TNF- α	-7.4	233	-12	69	18	20	20	20
MOL011975	Notoptol	TNF- α	-8	1253	-5	82	28	23	23	23
MOL011931	Vitetrifolin E	TNF- α	-7.4	233	-12	69	18	20	20	20
MOL001956	Cnidilin	TNF- α	-8	1253	-5	82	28	21	21	21
MOL002565	Medicarpin	ALB	-8.1	2341	-28	15	40	20	20	20
MOL011975	Notoptol	ALB	-9.3	2341	-28	15	40	23	23	23
MOL011931	Vitetrifolin E	ALB	-7.4	1260	-35	-8	10	21	21	21
MOL001956	Cnidilin	ALB	-8.8	7244	-19	-12	-4	35	30	21
MOL002565	Medicarpin	VEGFA	-6.4	537	27	-23	15	20	20	20
MOL011975	Notoptol	VEGFA	-7.7	537	27	-23	15	23	23	23
MOL011931	Vitetrifolin E	VEGFA	-6.3	537	27	-23	15	21	21	21
MOL001956	Cnidilin	VEGFA	-6	548	19	-55	8	21	21	21
MOL002565	Medicarpin	EGFR	-7.5	555	-52	2	24	20	20	20
MOL011975	Notoptol	EGFR	-8.2	643	-64	-7	31	23	23	23
MOL011931	Vitetrifolin E	EGFR	-7.2	555	-52	2	24	21	21	21
MOL001956	Cnidilin	EGFR	-7.8	643	-64	-7	31	21	21	21

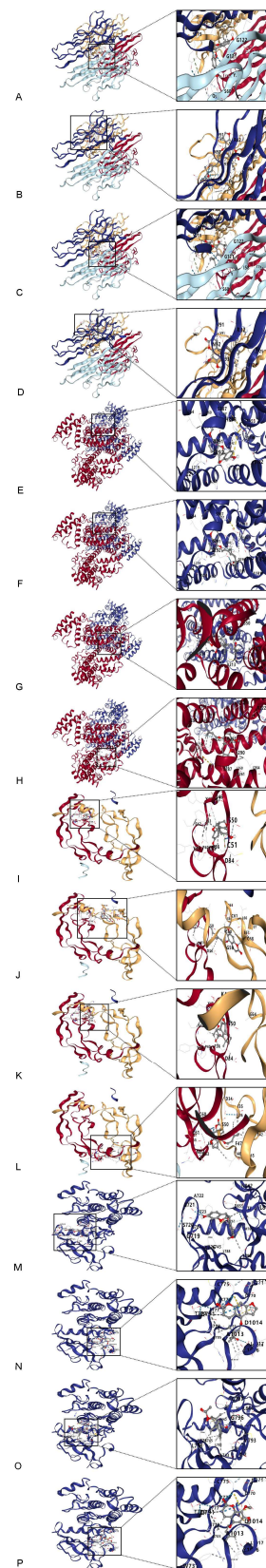


Figure 7. Simulation maps of docking. (A–D) TNF- α docking medicarpin, notopectol, vitetrifolin E, cnidilin; (E–H) ALB docking medicarpin, notopectol, vitetrifolin E, cnidilin; (I–L) VEGFA docking medicarpin, notopectol, vitetrifolin E, cnidilin; (M–P) EGFR docking medicarpin, notopectol, vitetrifolin E, cnidilin.

4. Discussion

AS is a prevalent inflammatory autoimmune disease that mostly affects the joints of the spine and causes significant persistent pain [1]. The inflammatory response and antigen presentation are important to our current understanding of its etiology [2]. The exact process through which QHSSD treats AS is currently unknown. For this reason, we investigated the potential mechanism of QHSSD in the treatment of AS using network pharmacology and molecular docking approaches.

In this study, the chemical compositions of the herbs in QHSSD were initially examined. After constructing the component–target network, the high-degree chemical components were discovered to be linked to inflammatory control. Medicarpin, for example, prevented changes in cytokine levels by downregulating pro-inflammatory cytokines including TNF- α , IL6, and IL17A [20]. By suppressing TH-17 and boosting Treg cells, medicarpin also prevented cartilage breakdown and bone erosion. As a result, the pro-inflammatory milieu of osteoclast production and bone degradation has been replaced with an anti-inflammatory environment that suppresses osteoclast formation [21]. Notoptol is a kind of coumarin with anti-inflammatory and analgesic properties, as well as the ability to stimulate melanin formation [22,23]. This suggests that QHSSD's treatment of AS may be carried out through a multi-component intervention in inflammation.

Next, we built a PPI network for the common potential targets (Figure 4A). The 193 target proteins do not operate individually. The connections between them revealed that they collaborate to co-regulate. The top 20 target proteins were chosen to build 3D bar graphs (Figure 4B) after being sorted by degree from largest to smallest. The correlation of these potential targets in the treatment of AS was supported by previous research.

For example, TNF- α , a pro-inflammatory cytokine, is primarily produced by activated macrophages and monocytes in response to injury [24]. TNF- α expression was higher in sacroiliac joint biopsies and plasma from AS patients, implying that TNF- α is implicated in the inflammatory process of AS [25–27]. In an inflammatory environment, TNF- α reduced miR-335-5p expression increased DKK1 expression to promote osteogenic differentiation [28]. Anti-TNF- α medication reduced the number of circulating pro-inflammatory immune cells such as Th17 and Tfh in AS patients and improved pain, tiredness, edema, and stiffness [23,29–31]. As a result, inhibitors of TNF- α , such as infliximab, enalapril, and adalimumab, are frequently used in AS patients and are safe and efficacious [32–34].

ALB is a plasma protein that keeps colloid pressure in check and transports free fatty acids, drug metabolites, and bilirubin. Inflammation has been shown to alter ALB production. For example, ALB levels dropped in acute malnutrition, chronic inflammation, and autoimmune disorders [35–37]. As a result, CRP/ALB has been recognized as a novel indicator for assessing inflammation levels in oncological and rheumatic immunological illnesses. This indicator was also included in the rheumatoid arthritis disease score [38–40]. ALB reflects a patient's nutritional state and the internal inflammatory response in people with AS. ALB levels are reduced when patients with ankylosing spondylitis present with various clinical signs and symptoms of kidney disease. [41].

VEGFA is produced primarily by macrophages and synoviocytes and acts selectively on endothelial cells. It is regarded as a crucial element in angiogenesis [42]. Angiogenesis and synovitis are both common features of rheumatic illnesses. Synovitis is caused by the formation of new blood vessels from existing ones. Synovitis in patients with AS is marked by increased vascularity and VEGFA levels. This implies that the vascular system has a role in the development of AS [43–47]. VEGFA is involved in practically every step of angiogenesis, boosting inflammatory levels as new blood vessels provide nutrients and oxygen [46]. One theory that has been proposed to explain new bone development in AS is angiogenesis. Angiogenesis is required not just for new bone production, but also for sacroiliitis and colitis, which are two AS symptoms. VEGFA is thought to play a key role in this process [47]. VEGFA, which is closely related to angiogenin, was found to be expressed in early inflammatory arthritis in several investigations [48]. VEGFA is thought to play

a role in the control of these processes during the pathogenesis of early AS. VEGFA and TNF- α have been found to influence the differentiation of synovial fibroblasts to promote new bone growth into osteoblasts in AS patients [49]. As a result, VEGFA plays a role in the therapy of AS by influencing angiogenesis.

EGFR is frequently regarded as a star gene in oncological disease, and it often plays a key role in tumor growth [50]. Serum levels of EGFR proteins have been found to be considerably higher in rheumatic disorders such as rheumatoid arthritis [51]. In rheumatoid arthritis, EGFR inhibitors have been found to suppress osteoclastogenesis in synovial fibroblasts and human primary endothelium cells, preventing synovitis [52]. It has also been discovered that EGFR can prevent the PI3K/AKT/mTOR signaling cascade from becoming activated, hence postponing inflammation [53]. To summarize, the QHSSD treatment of AS may, through numerous potential targets, influence inflammation and angiogenesis.

We elected to undertake GO function and KEGG enrichment analysis of the potential targets in PPI to further investigate the mechanism of action. Biological activities such as inflammatory response and protein phosphorylation were shown to be enhanced. It is possible that QHSSD is involved in the regulation of inflammation and protein phosphorylation, which could be useful in treating AS. Inflammation-related pathways, such as the PI3K-AKT and TNF pathways, were enriched. According to the enrichment count value, the MAPK signaling pathway could be the key pathway. As a result, we focused on the AS-related potential targets of the MAPK signaling pathway (Figure 8). TNF- α may activate the downstream MAPK pathway to further regulate the expression of MMP-1 and MMP-3 to exert pro-inflammatory effects; it could also activate MSK1 and MSK2 to mediate MAPK downstream signal transduction [54]. EGFR is a type of FTK whose overexpression increases the mRNA and protein expression levels of HRas, Raf1, MEK2, and c-Myc, which are key genes or downstream targets in the MAPK pathway [55]. Pharmacological studies have found that QHSSD also reduces the phosphorylation of mitogen-activated protein kinase (MAPK) and cAMP response element binding protein (CREB). MAPK and CREB are involved in the MAPK pathway and have anti-inflammatory and analgesic properties [56]. This also suggests that the MAPK pathway may be important in QHSSD's therapy of AS. In summary, QHSSD may interfere with the MAPK pathway by interfering with TNF- α , MAPK, CREB, and other mediated proteins.

One study has suggested that QHSSD may control TP53, VEGFA, EGFR, TNF, and NOS3, providing anti-inflammatory and antioxidant effects, while inhibiting cell proliferation and angiogenesis to intervene in rheumatoid arthritis [57]. Like ankylosing spondylitis, rheumatoid arthritis is also an autoimmune disease, and its pathogenesis also involves inflammation and angiogenesis [58]. Our study is therefore similar to the core potential target results derived from the abovementioned study. However, there are still some differences in both the core chemical active components and the core potential targets, suggesting that network pharmacology and molecular docking techniques have some specificity and are valuable for the screening of active drug components and core targets.

Molecular docking was used to evaluate four key target proteins (TNF- α , ALB, VEGFA, and EGFR) and chemical compounds, including medicarpin, notoptol, vitetrifolin E, and cnidilin. All docking Vina scores were less than -5 , meaning that the chemical components of QHSSD can bind to AS-related proteins on their own. This suggests that the pharmacological mechanism of QHSSD for the treatment of AS is multi-component and multi-target.

It is important to mention that this research has several limitations. Firstly, the chemical components and potential targets were acquired from databases. Therefore, the prediction ability and accuracy of the results are dependent on the databases' quality. Secondly, this study employed a data mining method that necessitates clinical trials and animal experiments to verify the findings.

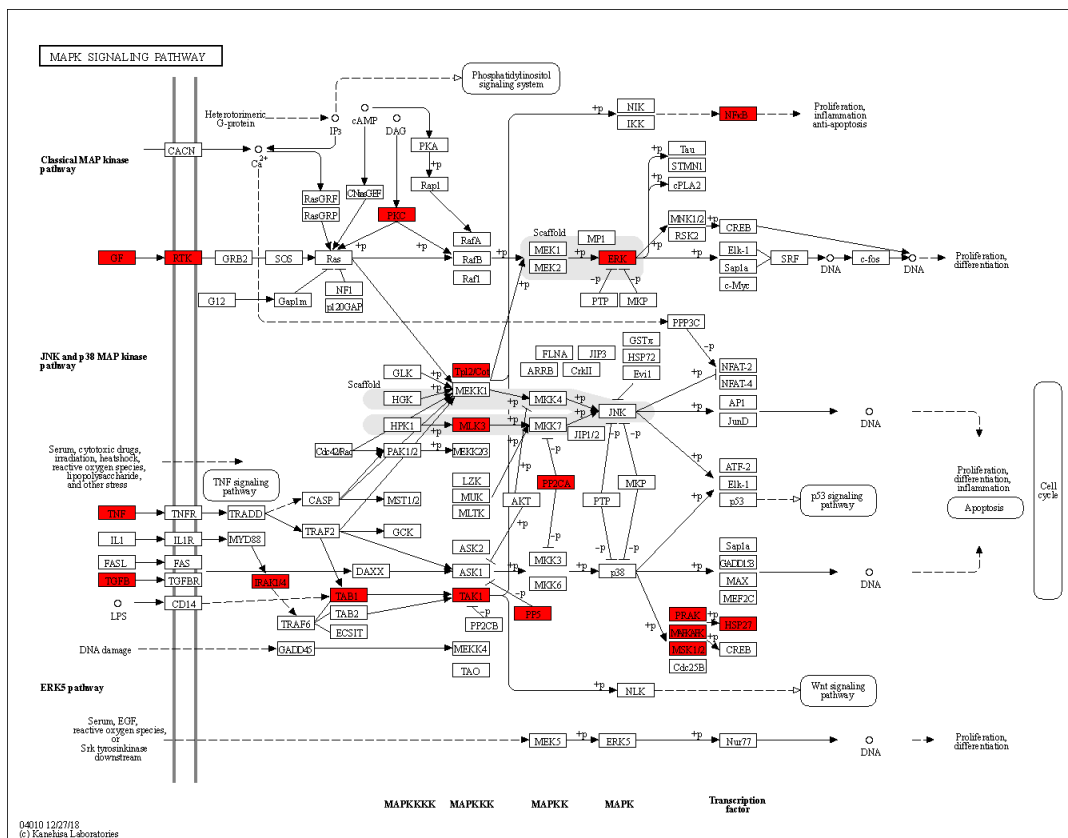


Figure 8. Mechanism of action of QHSSD in interfering with MAPK signaling pathway. Highlighted potential targets mediate MAPK signaling pathways to intervene in inflammation and angiogenesis.

5. Conclusions

To summarize, based on network pharmacology and molecular docking, this study investigated the pharmacological mechanism of QHSSD for the treatment of AS. The chemical compositions, potential targets, and pathways involved in the QHSSD treatment of AS were successfully predicted. Medicarpin, notoptol, vitetrifolin E, and cnidilin may be the main components of QHSSD for the treatment of AS, and TNF- α , ALB, VEGFA, and EGFR may be the main potential targets of QHSSD for the treatment of AS. Moreover, QHSSD can treat AS by influencing inflammation and angiogenesis via various pathways, e.g., MAPK.

Overall, this study focused on the multi-component, multi-target, and multi-pathway nature of QHSSD’s treatment of AS and its pharmacological mechanism. It provides a foundation for subsequent experiments and a reliable basis for drug selection in the treatment of AS.

Supplementary Materials: The following supporting information can be downloaded at: <https://www.mdpi.com/article/10.3390/pr10081487/s1> Table S1: ADME characteristic information of 154 chemical components. Table S2: A total, 193 common targets of QHSSD and AS.

Author Contributions: Conceptualization and methodology, S.L. and S.T.; software and visualization, X.X., W.L., and J.Z.; validation, data curation, and formal analysis, S.L. and X.Z.; investigation, X.X. and W.L.; writing—original draft preparation, S.L. and S.T.; supervision, project administration, and writing—review and editing, S.T. All authors have read and agreed to the published version of the manuscript.

Funding: This research was funded by The National Science Foundation of China, grant number 81860840, and Innovative Research Projects for Postgraduate Students in Hainan Province, China, grant number Qhys 2021-360.

Institutional Review Board Statement: Not applicable.

Informed Consent Statement: Not applicable.

Data Availability Statement: All data generated or analyzed during this study are included in this published article (and in the Supplementary Materials).

Acknowledgments: This study was conducted with the support of a research grant from Hainan Medical University in 2022.

Conflicts of Interest: The authors declare no conflict of interest.

Abbreviations

TCM, Traditional Chinese Medicine; QHSSD, Qianghuo Shengshi decoction; AS, ankylosing spondylitis; TCMSF, Traditional Chinese Medicine Systematic Pharmacology Database and Analysis Platform; OMIM, The Online Human Mendelian Inheritance Database; GO, gene ontology; KEGG, Kyoto Encyclopedia of Genes and Genomes; EGFR, epidermal growth factor receptor; TNF- α , tumor necrosis factor-alpha; ALB, serum albumin; VEGFA, vascular endothelial growth factor A; QH, Qianghuo; DH, Duhuo; CX, Chuanxiong; GB, Gaoben; FF, Fangfeng; MJZ, Manjingzi; GC, GanCao; ADME, absorption, distribution, metabolism, and efflux; DL, drug-like; OB, oral bioavailability; BP, biological process; CC, cellular component; MF, molecular function; PPI, protein-protein interaction; STRING, Search Tool for the Retrieval of Interacting Genes/Proteins database.

References

1. Braun, J.; Sieper, J. Ankylosing spondylitis. *Lancet* **2007**, *369*, 1379–1390. [[CrossRef](#)]
2. Zhu, W.; He, X.; Cheng, K.; Zhang, L.; Chen, D.; Wang, X.; Qiu, G.; Cao, X.; Weng, X. Ankylosing spondylitis: Etiology, pathogenesis, and treatments. *Bone Res.* **2019**, *7*, 22. [[CrossRef](#)] [[PubMed](#)]
3. Wang, J.; Li, H.; Wang, J.; Gao, X. Association between ERAP1 gene polymorphisms and ankylosing spondylitis susceptibility in Han population. *Int. J. Clin. Exp. Pathol.* **2015**, *8*, 11641–11646.
4. Zochling, J.; van der Heijde, D.; Burgos-Vargas, R.; Collantes, E., Jr.; Davis, J.C.; Dijkmans, B.; Dougados, M.; Géher, P.; Inman, R.; Khan, M.A.; et al. ASAS/EULAR recommendations for the management of ankylosing spondylitis. *Ann. Rheum. Dis.* **2006**, *65*, 442–452. [[CrossRef](#)] [[PubMed](#)]
5. Salaffi, F.; Carotti, M.; Gasparini, S.; Intorcia, M.; Grassi, W. The health-related quality of life in rheumatoid arthritis, ankylosing spondylitis, and psoriatic arthritis: A comparison with a selected sample of healthy people. *Health Qual. Life Outcomes* **2009**, *7*, 25. [[CrossRef](#)]
6. Overman, C.L.; Kool, M.B.; Da Silva, J.; Geenen, R. The prevalence of severe fatigue in rheumatic diseases: An international study. *Clin. Rheumatol.* **2016**, *35*, 409–415. [[CrossRef](#)]
7. Brophy, S.; Davies, H.; Dennis, M.S.; Cooksey, R.; Husain, M.J.; Irvine, E.; Siebert, S. Fatigue in ankylosing spondylitis: Treatment should focus on pain management. *Semin. Arthritis Rheum.* **2013**, *42*, 361–367. [[CrossRef](#)]
8. Braun, J.; van den Berg, R.; Baraliakos, X.; Boehm, H.; Burgos-Vargas, R.; Estévez, E.C.; Dagfinrud, H.; Dijkmans, B.; Dougados, M.; Emery, P.; et al. 2010 update of the ASAS/EULAR recommendations for the management of ankylosing spondylitis. *Ann. Rheum. Dis.* **2011**, *70*, 896–904. [[CrossRef](#)]
9. Bahadur, S.; Keshri, L.; Pathak, K. Adverse drug reactions and safety considerations of NSAIDs: Clinical analysis. *Curr. Drug Saf.* **2011**, *6*, 310–317. [[CrossRef](#)] [[PubMed](#)]
10. Tao, W.; Xu, X.; Wang, X.; Li, B.; Wang, Y.; Li, Y.; Yang, L. Network pharmacology-based prediction of the active ingredients and potential targets of Chinese herbal *Radix Curcumae* formula for application to cardiovascular disease. *J. Ethnopharmacol.* **2013**, *145*, 1–10. [[CrossRef](#)] [[PubMed](#)]
11. Xu, X.; Zhang, W.; Huang, C.; Li, Y.; Yu, H.; Wang, Y.; Duan, J.; Ling, Y. A novel chemometric method for the prediction of human oral bioavailability. *Int. J. Mol. Sci.* **2012**, *13*, 6964–6982. [[CrossRef](#)]
12. Tian, S.; Wang, J.; Li, Y.; Li, D.; Xu, L.; Hou, T. The application of *in silico* drug-likeness predictions in pharmaceutical research. *Adv. Drug Deliv. Rev.* **2015**, *86*, 2–10. [[CrossRef](#)]
13. Daina, A.; Michielin, O.; Zoete, V. SwissTargetPrediction: Updated data and new features for efficient prediction of protein targets of small molecules. *Nucleic Acids Res.* **2019**, *47*, W357–W364. [[CrossRef](#)]
14. Fishilevich, S.; Zimmerman, S.; Kohn, A.; Stein, T.I.; Olender, T.; Kolker, E.; Safran, M.; Lancet, R. Genic insights from integrated human proteomics in GeneCards. *Database (Oxf.)* **2016**, *2016*, 30. [[CrossRef](#)] [[PubMed](#)]
15. Amberger, J.S.; Hamosh, A. Searching Online Mendelian Inheritance in Man (OMIM): A Knowledgebase of Human Genes and Genetic Phenotypes. *Curr. Protoc. Bioinform.* **2017**, *58*, 1.2.1–1.2.12. [[CrossRef](#)] [[PubMed](#)]

16. Piñero, J.; Saüch, J.; Sanz, F.; Furlong, L.I. The DisGeNET cytoscape app: Exploring and visualizing disease genomics data. *Comput. Struct. Biotechnol. J.* **2021**, *19*, 2960–2967. [[CrossRef](#)]
17. Szklarczyk, D.; Gable, A.L.; Nastou, K.C.; Lyon, D.; Kirsch, R.; Pyysalo, S.; Doncheva, N.T.; Legeay, M.; Fang, T.; Bork, P.; et al. The STRING database in 2021: Customizable protein-protein networks, and functional characterization of user-uploaded gene/measurement sets. *Nucleic Acids Res.* **2021**, *49*, D605–D612, Published Correction Appears in *Nucleic Acids Res.* **2021**, *49*, 10800. [[CrossRef](#)] [[PubMed](#)]
18. Huang, D.W.; Sherman, B.T.; Tan, Q.; Kir, J.; Liu, D.; Bryant, D.; Guo, Y.; Stephens, R.; Baseler, M.W.; Lane, H.C.; et al. DAVID Bioinformatics Resources: Expanded annotation database and novel algorithms to better extract biology from large gene lists. *Nucleic Acids Res.* **2007**, *35*, W169–W175. [[CrossRef](#)]
19. Liu, Y.; Grimm, M.; Dai, W.T.; Hou, M.-C.; Xiao, Z.-X.; Cao, Y. CB-Dock: A web server for cavity detection-guided protein-ligand blind docking. *Acta Pharm. Sin.* **2020**, *41*, 138–144. [[CrossRef](#)]
20. Tyagi, A.M.; Gautam, A.K.; Kumar, A.; Srivastava, K.; Bhargavan, B.; Trivedi, R.; Saravanan, S.; Yadav, D.K.; Singh, N.; Pollet, C.; et al. Medicarpin inhibits osteoclastogenesis and has nonestrogenic bone conserving effect in ovariectomized mice. *Mol. Cell Endocrinol.* **2010**, *325*, 101–109. [[CrossRef](#)]
21. Mansoori, M.N.; Raghuvanshi, A.; Shukla, P.; Awasthi, P.; Trivedi, R.; Goel, A.; Singh, D. Medicarpin prevents arthritis in post-menopausal conditions by arresting the expansion of TH17 cells and pro-inflammatory cytokines. *Int. Immunopharmacol.* **2020**, *82*, 106299. [[CrossRef](#)]
22. Azietaku, J.T.; Ma, H.; Yu, X.-A.; Li, J.; Oppong, M.B.; Cao, J.; An, M.; Chang, Y.-X. A review of the ethnopharmacology, phytochemistry and pharmacology of *Notopterygium incisum*. *J. Ethnopharmacol.* **2017**, *202*, 241–255. [[CrossRef](#)] [[PubMed](#)]
23. Matsuda, H.; Hirata, N.; Kawaguchi, Y.; Yamazaki, M.; Naruto, S.; Shibano, M.; Taniguchi, M.; Baba, K.; Kubo, M. Melanogenesis stimulation in murine b16 melanoma cells by umberiferae plant extracts and their coumarin constituents. *Biol. Pharm. Bull.* **2005**, *28*, 1229–1233. [[CrossRef](#)]
24. van der Heijde, D.; Kivitz, A.; Schiff, M.H.; Sieper, J.; Dijkmans, B.A.C.; Braun, J.; Dougados, M.; Reveille, J.D.; Wong, R.L.; Kupper, H.; et al. Efficacy and safety of adalimumab in patients with ankylosing spondylitis: Results of a multicenter, randomized, double-blind, placebo-controlled trial. *Arthritis Rheum.* **2006**, *54*, 2136–2146. [[CrossRef](#)]
25. Braun, J.; Bollow, M.; Neure, L.; Seipelt, E.; Seyrekbasan, F.; Herbst, H.; Eggens, U.; Distler, A.; Sieper, J. Use of immunohistologic and in situ hybridization techniques in the examination of sacroiliac joint biopsy specimens from patients with ankylosing spondylitis. *Arthritis Rheum.* **1995**, *38*, 499–505. [[CrossRef](#)] [[PubMed](#)]
26. Sveaas, S.H.; Berg, I.J.; Provan, S.; Semb, A.; Olsen, I.C.; Ueland, T.; Aukrust, P.; Vøllestad, N.; Hagen, K.; Kvien, T.; et al. Circulating levels of inflammatory cytokines and cytokine receptors in patients with ankylosing spondylitis: A cross-sectional comparative study. *Scand. J. Rheumatol.* **2015**, *44*, 118–124. [[CrossRef](#)] [[PubMed](#)]
27. Zambrano-Zaragoza, J.F.; Gutiérrez-Franco, J.; Durán-Avelar, M.J.; Vibanco-Pérez, N.; Ortiz-Martínez, L.; Ayón-Pérez, M.F.; Vázquez-Reyes, A.; Agraz-Cibrián, J.M. Neutrophil extracellular traps and inflammatory response: Implications for the immunopathogenesis of ankylosing spondylitis. *Int. J. Rheum. Dis.* **2021**, *24*, 426–433. [[CrossRef](#)]
28. Li, S.; Yin, Y.; Yao, L.; Lin, Z.; Sun, S.; Zhang, J.; Li, X. TNF- α treatment increases DKK1 protein levels in primary osteoblasts via upregulation of DKK1 mRNA levels and downregulation of miR-335-5p. *Mol. Med. Rep.* **2020**, *22*, 1017–1025. [[CrossRef](#)]
29. Wu, Q.; Inman, R.D.; Davis, K.D. Tumor necrosis factor inhibitor therapy in ankylosing spondylitis: Differential effects on pain and fatigue and brain correlates. *Pain* **2015**, *156*, 297–304. [[CrossRef](#)] [[PubMed](#)]
30. Chen, R.; Qian, H.; Yuan, X.; Chen, S.; Liu, Y.; Wang, B.; Shi, G. Immunological Changes in Peripheral Blood of Ankylosing Spondylitis Patients during Anti-TNF- α Therapy and Their Correlations with Treatment Outcomes. *J. Immunol. Res.* **2021**, *2021*, 1017938. [[CrossRef](#)] [[PubMed](#)]
31. Maxwell, L.J.; Zochling, J.; Boonen, A.; Chen, S.; Liu, Y.; Wang, B.; Shi, G. TNF-alpha inhibitors for ankylosing spondylitis. *Cochrane Database Syst. Rev.* **2015**, *4*, CD005468. [[CrossRef](#)]
32. Lata, M.; Hettinghouse, A.S.; Liu, C.J. Targeting tumor necrosis factor receptors in ankylosing spondylitis. *Ann. N. Y. Acad. Sci.* **2019**, *1442*, 5–16. [[CrossRef](#)]
33. Tahir, H. Therapies in ankylosing spondylitis—from clinical trials to clinical practice. *Rheumatology (Oxford)* **2018**, *57* (Suppl. S6), vi23–vi28. [[CrossRef](#)]
34. Hou, L.Q.; Jiang, G.X.; Chen, Y.F.; Yang, X.-M.; Meng, L.; Xue, M.; Liu, X.-G.; Chen, X.-C.; Li, X. The Comparative Safety of TNF Inhibitors in Ankylosing Spondylitis—a Meta-Analysis Update of 14 Randomized Controlled Trials. *Clin. Rev. Allergy Immunol.* **2018**, *54*, 234–243. [[CrossRef](#)]
35. Ruot, B.; Béchereau, F.; Bayle, G.; Breuillé, D.; Obled, C. The response of liver albumin synthesis to infection in rats varies with the phase of the inflammatory process. *Clin. Sci.* **2002**, *102*, 107–114. [[CrossRef](#)]
36. Zhong, Z.; Huang, Y.; Liu, Y.; Chen, J.; Liu, M.; Huang, Q.; Zheng, S.; Guo, X.; Deng, W.; Li, T. Correlation between C-Reactive Protein to Albumin Ratio and Disease Activity in Patients with Axial Spondyloarthritis. *Dis. Markers* **2021**, *2021*, 6642486. [[CrossRef](#)]
37. Gabay, C.; Kushner, I. Acute-phase proteins and other systemic responses to inflammation. *N. Engl. J. Med.* **1999**, *340*, 448–454, Published Correction Appears in *N. Engl. J. Med.* **1999**, *340*, 1376. [[CrossRef](#)]
38. Liu, M.; Huang, Y.; Huang, Z.; Zhong, Z.; Deng, W.; Huang, Z.; Huang, Q.; Li, T. The role of fibrinogen to albumin ratio in ankylosing spondylitis: Correlation with disease activity. *Clin. Chim. Acta* **2020**, *505*, 136–140. [[CrossRef](#)]

39. Yang, W.M.; Zhang, W.H.; Ying, H.Q.; Xu, Y.-M.; Zhang, J.; Min, Q.-H.; Huang, B.; Lin, J.; Chen, J.-J.; Wang, X.-Z. Two new inflammatory markers associated with disease activity score-28 in patients with rheumatoid arthritis: Albumin to fibrinogen ratio and C-reactive protein to albumin ratio. *Int. Immunopharmacol.* **2018**, *62*, 293–298. [[CrossRef](#)]
40. Kinoshita, A.; Onoda, H.; Imai, N.; Iwaku, A.; Oishi, M.; Tanaka, K.; Fushiya, N.; Koike, K.; Nishino, H.; Matsushima, M. The C-reactive protein/albumin ratio, a novel inflammation-based prognostic score, predicts outcomes in patients with hepatocellular carcinoma. *Ann. Surg. Oncol.* **2015**, *22*, 803–810. [[CrossRef](#)]
41. Wu, Y.; Zhang, G.; Wang, N.; Xue, Q. Risk Factors of Renal Involvement Based on Different Manifestations in Patients with Ankylosing Spondylitis. *Kidney Blood Press. Res.* **2018**, *43*, 367–377. [[CrossRef](#)] [[PubMed](#)]
42. Lu, J.; Kasama, T.; Kobayashi, K.; Yoda, Y.; Shiozawa, F.; Hanyuda, M.; Negishi, M.; Ide, H.; Adachi, M. Vascular endothelial growth factor expression and regulation of murine collagen-induced arthritis. *J. Immunol.* **2000**, *164*, 5922–5927. [[CrossRef](#)] [[PubMed](#)]
43. Drouart, M.; Saas, P.; Billot, M.; Cedoz, J.; Tiberghien, P.; Wendling, D.; Toussiro, E. High serum vascular endothelial growth factor correlates with disease activity of spondylarthropathies. *Clin. Exp. Immunol.* **2003**, *132*, 158–162. [[CrossRef](#)]
44. Lin, T.T.; Lu, J.; Qi, C.Y.; Yuan, L.; Li, X.-L.; Xia, L.-P.; Shen, H. Elevated serum level of IL-27 and VEGF in patients with ankylosing spondylitis and associate with disease activity. *Clin. Exp. Med.* **2015**, *15*, 227–231. [[CrossRef](#)]
45. Carvalho, J.F.; Blank, M.; Shoenfeld, Y. Vascular endothelial growth factor (VEGF) in autoimmune diseases. *J. Clin. Immunol.* **2007**, *27*, 246–256. [[CrossRef](#)]
46. Distler, J.H.; Hirth, A.; Kurowska-Stolarska, M.; Gay, R.E.; Gay, S.; Distler, O. Angiogenic and angiostatic factors in the molecular control of angiogenesis. *Q. J. Nucl. Med.* **2003**, *47*, 149–161.
47. Yamamoto, T. Angiogenic and inflammatory properties of psoriatic arthritis. *ISRN Dermatol.* **2013**, *2013*, 630620. [[CrossRef](#)]
48. Fearon, U.; Griosos, K.; Fraser, A.; Reece, R.; Emery, P.; Jones, P.F.; Veale, D. Angiopoietins, growth factors, and vascular morphology in early arthritis. *J. Rheumatol.* **2003**, *30*, 260–268.
49. Liu, K.; He, Q.; Tan, J.; Liao, G. Expression of TNF- α , VEGF, and MMP-3 mRNAs in synovial tissues and their roles in fibroblast-mediated osteogenesis in ankylosing spondylitis. *Genet. Mol. Res.* **2015**, *14*, 6852–6858. [[CrossRef](#)]
50. Harrison, P.T.; Vyse, S.; Huang, P.H. Rare epidermal growth factor receptor (EGFR) mutations in non-small cell lung cancer. *Semin. Cancer Biol.* **2020**, *61*, 167–179. [[CrossRef](#)] [[PubMed](#)]
51. Huang, C.-M.; Chen, H.-H.; Chen, D.-C.; Huang, Y.-C.; Liu, S.-P.; Lin, Y.-J.; Chang, Y.-Y.; Lin, H.-W.; Chen, S.-Y.; Tsai, F.-J. Rheumatoid arthritis is associated with rs17337023 polymorphism and increased serum level of the EGFR protein. *PLoS ONE* **2017**, *12*, e0180604. [[CrossRef](#)] [[PubMed](#)]
52. Killock, D. Experimental arthritis: Targeting EGFR to fight synovitis. *Nat. Rev. Rheumatol.* **2012**, *8*, 247. [[CrossRef](#)]
53. Jiang, L.; Zhou, X.; Xu, K.; Hu, P.; Bao, J.; Li, J.; Zhu, J.; Wu, L. miR-7/EGFR/MEGF9 axis regulates cartilage degradation in osteoarthritis via PI3K/AKT/mTOR signaling pathway. *Bioengineered* **2021**, *12*, 8622–8634. [[CrossRef](#)]
54. Colomb, F.; Vidal, O.; Bobowski, M.; Krzewinski-Recchi, M.-A.; Harduin-Lepers, A.; Mensier, E.; Jaillard, S.; Lafitte, J.-J.; Delannoy, P.; Groux-Degroote, S. TNF induces the expression of the sialyltransferase ST3Gal IV in human bronchial mucosa via MSK1/2 protein kinases and increases FliD/sialyl-Lewis(x)-mediated adhesion of *Pseudomonas aeruginosa*. *Biochem. J.* **2014**, *457*, 79–87. [[CrossRef](#)] [[PubMed](#)]
55. Hu, N.; Wang, C.; Wang, B.; Wang, L.; Huang, J.; Wang, J.; Li, C. Qianghuo Shengshi decoction exerts anti-inflammatory and analgesic via MAPKs/CREB signaling pathway. *J. Ethnopharmacol.* **2022**, *284*, 114776. [[CrossRef](#)]
56. Wu, Y.; Xiao, H.; Pi, J.; Zhang, H.; Pan, A.; Pu, Y.; Liang, Z.; Shen, J.; Du, J. EGFR promotes the proliferation of quail follicular granulosa cells through the MAPK/extracellular signal-regulated kinase (ERK) signaling pathway. *Cell Cycle* **2019**, *18*, 2742–2756. [[CrossRef](#)] [[PubMed](#)]
57. Zeng, Z.; Hu, J.; Jiang, J.; Xiao, G.; Yang, R.; Li, S.; Li, Y.; Huang, H.; Zhong, H.; Bi, X. Network Pharmacology and Molecular Docking-Based Prediction of the Mechanism of Qianghuo Shengshi Decoction against Rheumatoid Arthritis. *Biomed. Res. Int.* **2021**, *2021*, 6623912. [[CrossRef](#)]
58. Scott, D.L.; Wolfe, F.; Huizinga, T.W.J. Rheumatoid arthritis. *Lancet* **2010**, *376*, 1094–1108. [[CrossRef](#)]